

Manuskript für Marine Geology

**Clay Mineral Distribution  
in Surface Sediments  
of the South Atlantic:  
Sources, Transport,  
and Relation to Oceanography**

Rainer Petschick<sup>1) 2)</sup>, Gerhard Kuhn<sup>1)</sup>, and Franz Gingele<sup>1)</sup>

with 13 Figures, 1 Table

<sup>1)</sup> Alfred-Wegener-Institut für Polar- und Meeresforschung, Columbusstr.,  
27515 Bremerhaven, Germany

<sup>2)</sup> Present Adress: Geologisch-Paläontologisches Institut, J.W.Goethe  
University, Senckenberganlage 32-34, 60054 Frankfurt am Main, Germany

## Abstract

850 surface samples mostly from abyssal sediments of the South Atlantic and the Antarctic Ocean were investigated for clay content and composition. Maps of relative clay mineral content were compiled, which improve previous maps by showing more details, especially at high latitudes. Large-scaled relations regarding the origin and transport paths of detrital clay are revealed. Near submarine volcanoes of the Antarctic Ocean (South Sandwich, Bouvet Island) smectite contents exhibit distinct maxima, which is ascribed to the erosion of altered basalts and volcanic glasses. Other areas of high smectite concentration are observed in abyssal regions, primarily derived from southernmost America and from minor sources in Southwest Africa. The illite distribution can be subdivided into five major zones including two maxima revealing both South African and Antarctic sources. A particularly high amount of Fe- and Mg-rich illites are observed close to East Antarctica derived from biotite bearing crystalline rocks and transported to the west by the East Antarctic Coastal current. Chlorites and well-crystallized illites are typical minerals enriched within the Subantarctic and Polarfrontal-Zone but of minor importance off East Antarctica. Kaolinites dominate the clay mineral assemblage in low latitudes, where the source rocks on land (West Africa, Brazil) are mainly affected by intensive chemical weathering. Surprisingly, a slight increase of kaolinite is observed in the Enderby Basin and near the Filchner-/Ronne Iceshelf.

The South Atlantic can be subdivided into ten large-scaled clay facies zones with characteristic possible source regions and transport paths. Clay mineral assemblages of the largest part of the South Atlantic, especially of the western basins are dominated by chlorites and illites derived from the Antarctic Peninsula and southernmost America and supported by advection within the Circumantarctic Deep Water flow. In comparison, the role of the East Antarctic shield as a source area is only minor. Assemblages of the eastern basins north of 30°S are strongly influenced by African sources. They can be subdivided into three latitudinal zones of illite, smectite, and kaolinite enrichment controlled by weathering regimes on land and by a complex interaction of wind, river and deep ocean transport. In contrast, the clay contribution of South America to the deep ocean at low latitudes appears to be poor.

## 1. Introduction

Clay minerals are main constituents of most modern abyssal sediments. Their role as paleoclimatic and paleoceanographic indicators has been investigated world-wide by a number of contributors applying X-ray diffraction (XRD) techniques. In the South Atlantic the recent composition of clay detritus was obtained by Biscaye (1965) already 30 years ago and - as part of world-wide examinations - by Griffin et al. (1968), Rateev, et al. (1969), and Windom (1976). Compared to the abundance of studies dealing with recent distributions of clay minerals found along the surrounding continental margins, the available dataset published from South Atlantic deep-sea sites is still incomplete. Especially in the Atlantic part of the Antarctic Ocean the database is very poor.

All of the previous workers have shown that the Recent clay mineral distribution of the Atlantic Ocean is principally caused by the climatic and weathering zonation on adjacent land masses, implying that most of the clay minerals are of terrigenous origin (Chamley, 1989). On the other hand, the transport of clay particles to their deep sea deposition is controlled by a complex system of atmospheric, hydrographic and topographic conditions. In areas of low vegetation, like the arid regions of North and Southwest Africa, wind transport is the major process, which supplies terrigenous matter to the ocean (Prospero, 1981). The dust-loadings transported by NE- and SE-trades amount to  $0.13 \text{ mg/m}^3$  of air (Chester et al., 1972). Along the African coast, the distribution of suspended clayey particles (Behairy et al., 1975) as well as aerosols show a clear relation to the clay mineral provinces of the source regions on land (Chester et al., 1972; Aston et al., 1973). If humid conditions prevail, the near-shore clay mineral input is controlled by river systems, e.g. near the mouths of the Zaire (Eisma et al., 1978; Van der Gaast and Janssen, 1984) and Amazon Rivers (Baretto, et al., 1975; Gibbs, 1977). Here, kaolin minerals are usually the best indicators to record tropical and humid weathering processes as well as the intensity of river discharge.

A considerable amount of clay minerals are supplied to the South Atlantic by glaciomarine processes at the Antarctic Continental Margin. The physical weathering and erosion of source rocks by the inland ice sheet (Ehrmann et al., 1992) leads to mechanical crushing, but causes less degradation of phyllosilicates than observed elsewhere. Glacially affected clay mineral

associations generally mirror the composition of the source rocks directly. Clay minerals which are usually unstable under hydrolysis are well-preserved, such as chlorite or biotites. The main site of **sediment** input into the Antarctic Ocean is near the grounding line of the ice shelves, where material incorporated in the ice is released during melting, **thus** leading to suspensions with a high amount of fine-grained terrigenous matter (Anderson et al., 1980a). **Although very small mineral inclusions can even be observed in the snow at the South Pole (Kumai, 1976), the large Antarctic ice shelves are mostly accumulated from nearly dust-free snow.** Due to the barrier effect of the large Antarctic ice shelves the impact of ice-rafting upon the clay sedimentation in the Southern Ocean in Recent sediments is relative minor. Pure ice-rafted material (IRD) which is usually poor in clay components (Anderson et al., 1980b) is mainly enriched on the Antarctic shelves and continental margins (Anderson et al., 1980a, Elverhøi and Roaldset, 1983; Grobe, 1986; Grobe et al., 1993). In the deep sea IRD appears more episodically, but can be traced to subpolar parts of the Southern Ocean.

In deep ocean basins advective transport of clay mineral detritus within the deep water column becomes more important. Near the continental slopes much of the clay material can be derived from turbidity currents **and local, dense thermohaline underflows (Kuhn and Weber, 1993).** With increasing distance from source areas thermohaline current systems determine the clay composition within the sediment. Especially deep and bottom current activity cause a resuspension of clayey material within nepheloid layers as well as a horizontal drift in the scale of several thousands of nautical miles. In the Western South Atlantic basins, these processes are predominant, mainly triggered by the northward drifting cold water masses. In the bottom layer of the Argentine Basin and the Antarctic Ocean more than 60 million metric tons of particulate loads are estimated by nephelometer measurements (Biscaye and Eitrem, 1977).

The use of abyssal clay mineral associations as tracers of source regions and as indicators of water mass fluctuations was first documented at the Vema channel between the Brazil and Argentine Basins. Chamley (1975, 1989) and in more detail, Jones (1984), found that the distribution of kaolinite and poorly-crystallized illite were strongly related to southwards flowing North Atlantic Deep Water (NADW). In contrast to Chamley, who assumed an advection of these material from low latitudes, Jones suggested a westerly source from

Brazil. Chlorite and well-crystallized illite-rich material was observed from water depths, where northward flowing Lower Circumantarctic Deep Water (LCDW), a mixture of Circumantarctic Water (CDW) and Weddell Sea Deep Water (WSDW) (according to the definition of Peterson and Withworth, 1989, and Reid, 1989) prevailed.

In this paper we try to improve the available knowledge on the Recent clay mineral distribution in the South Atlantic. With emphasis on the clay mineral assemblages of the Antarctic Ocean, which have been only poorly documented so far, we try to distinguish clay mineral provinces. Possible source areas are identified and the mode and direction of the clay mineral transport is related to oceanographic regimes.

## **2. Investigation area and sample distribution**

The investigation area stretches from 7°N to 78°S and from 70°W to 40°E (Fig. 1). Thus all topographic structures of the South Atlantic and its southern continuation are covered.

In the investigation area more than 850 samples were available for this study (Fig.1), collected during several cruises of *RV Polarstern* between 1985 and 1992 (ANT-IV/3, -IV/4, -V/2, -VI/3, -VIII/3, -VIII/6, -IX/2, -IX/3, -IX/4, -X/4, -X/6, -XI/2) and *RV Meteor* between 1988 and 1992 (M-6/6, M-9/4, M-12/1, M-20/2, M-23/1-3). About 70 surface samples, which were collected around the islands of South Orkney, South Georgia, and South Shetland by several Spanish expeditions in 1986 and 1987 (Fig. 1) (*Antartida*) were kindly provided by A. Barcena.

In the eastern part of the South Atlantic the sample distribution covers essential parts of the deep water masses, which are outlined by salinity isolines (Fig. 11b). Due to topographical constraints, the sample distribution in relation to water depth in the western part is more discontinuous.

## **3. Methods**

### *3.1. Sample preparation*

A large box corer, a multicorer, and a minicorer were used to obtain undisturbed samples of the upper centimeter of the sediment column on each station. Depending on availability, the amount of untreated sediment we used varied between 5 to 300 g. Some large samples were wet splitted into proportions of lower than 20 g. For disaggregation and removal of organic carbon, each sample was shaken in a 5% hydrogenic peroxide solution for 24 hours. After wet sieving of the sand (63 - 2000  $\mu\text{m}$   $\phi$ ), and gravel (2 - 6.3 mm  $\phi$ ) fractions, clay and silt was separated by Stoke's law settling method. Using 1% sodium pyrophosphate solution to avoid coagulation of clay size particles, 8 to 12 separation procedures were required. For samples rich in carbonate we used a 0.25‰  $\text{NH}_3$  solution as a dispersion agent. The clay (< 2  $\mu\text{m}$   $\phi$ ) suspensions were treated with  $\text{MgCl}_2$  to accelerate the sinking of clay particles as well as to provide a unique cation charging. The clay suspensions were washed and centrifuged at least two times with deionized water to remove free ions. All grain size fractions were dried at 50°C and weighed to calculate their share of the bulk sediment.

The clay fractions were carefully grinded in an agate mortar. Some clay samples with a high  $\text{CaCO}_3$  content were subsequently treated with 10% acetic acid. About 50 samples containing high amounts of amorphous opal-A (> 30%) from the high production zone at the Polarfront were leached for 30 minutes with 1 N sodium hydroxide at a maximum temperature of 80°C. Experiments with less aggressive 2 M sodium carbonate solution did not improve the removal of biogenic opal even after boiling. XRD comparisons with untreated material did not produce evidence for a statistical removal of any of the clay minerals, with the exception of a slight decrease in smectite contents (< 10%) in some samples. The leached clay fractions were furnished with the same  $\text{Mg}^{++}$  charging as the untreated material.

To support quantitative measurements an internal standard of 1 ml of a 0.4% molybdenite suspension (0.3  $\mu\text{m}$  grain-diameter) was added to a 40 mg clay sample before resuspension. According to Quakernaat (1970) the accuracy of molybdenite is lower than 7 to 10% of the actual content of a clay mineral. Talc often used as an internal standard (McManus, 1991) was not recommended,

because it was observed as a natural mineral in some of our samples and it can influence the 10 Å illite peak form.

For XRD measurements we used two types of texture preparations. If possible both were applied on each sample. For the first method, [used for semi-quantitative estimation of clay minerals](#), 40 mg of clay were dispersed in an ultrasonic cleaner, and sucked onto a Millipore membran filter (pore diameter 0.15  $\mu\text{m}$ ) by a vacuum filtration apparatus. After drying for 15 minutes at 50°C the clay cakes were transferred onto aluminium platelets with double-sided adhesive tape (see Ehrmann et al., 1992). This preparation technic leads to highly textured, low particle-size segregated clay films. Their thickness of about 50 to 100  $\mu\text{m}$  (10 mg/cm<sup>2</sup>) exceeds the 'infinite thickness' which is required for semi-quantitative determination of clay minerals (Drever, 1973; Moore and Reynolds, 1989; McManus, 1992).

About 30 clay samples did not provide sufficient material for vacuum filter cakes, especially after removal of carbonate or amorphous silica. In this case, and for comparison to the filter method, evaporated texture preparations were made from each sample. 0,5 ml of an ultrasonic-dispersed clay suspension containing 4 mg dry substance (usually taken as an aliquot of a suspension containing 10 or 20 mg clay) were pipetted directly on 3 cm<sup>2</sup> aluminium platelets. After drying clay film thicknesses reached only 10 to 15  $\mu\text{m}$  (about 1,5 mg/cm<sup>2</sup>), which is slightly lower than the 'infinite thickness' of our instrument. This quicker technique has the disadvantage of increasing the amount of material of small particle size on the surface. Nevertheless, comparing the results of both preparation techniques, [little](#) statistical differences of clay mineral amounts were observed. Only the smectite contents measured on evaporated preparations are more scattered than the corresponding values observed on vacuum filter cakes. [We primary used evaporated preparations for illite and smectite 'crystallinity' measurements \(see below\), which are more accurate than observed by filter cake preparations.](#)

### *3.2. XRD measurements*

All samples were measured with a Philips PW 1820 goniometer, using CoK $\alpha$  radiation (40 kV, 40 mA), equipped with an theta-circle-integrated automatic

divergence slit, a graphite monochromator, and an automatic sample changer. The XRD measurements were carried out by a step scan with 2 seconds counting time for each angle. At first, the 'air dried' sample ( $\approx 50\%$  constant humidity in air-conditioned measuring room) was counted between  $1 - 18^\circ 2\theta$ , step size  $0.02^\circ$ . After vaporisation with ethylene glycol at  $50^\circ\text{C}$  for at least 1 day, each sample was analysed between  $2 - 40^\circ 2\theta$ , with a step size of  $0.02^\circ$ . Subsequently the area between  $28$  and  $30.5^\circ 2\theta$  was measured with steps of  $0.005^\circ 2\theta$  to separate the (002) peak of kaoline minerals from (004) reflections of chlorite minerals (see below). Additional complete XRD scans were run on texture free preparations of selected clay fractions to discover **different** illite and smectite **types**.

### 3.2. Analysis of XRD diagrams

The count values were stored on a Digital Equipment PDP 11 workstation and transmitted to an Apple Macintosh personal computer. Using the graphically oriented computer program 'MacDiff' written by the first author of this paper, counts were automatically smoothed by an 17-term-filter (weighted means). XRD spectra were corrected to the d-value of (001) molybdenite and the base line was computed using a simple algorithm. If required each background was corrected graphically. Next, basal reflections were analysed by determining the d-value, intensity, integrated peak area ( $\Sigma$  of counts), and half-height-width. The possibility of interactive correction of base lines, peak edges and coinciding lines at any time during the analysis prevents incorrect recording of the peak data than without any control by the user.

For empirical qualitative and semi-quantitative considerations the lines of the following minerals were counted:

- Smectite (+ vermiculite + smectite-vermiculite mixed layer) at  $17 \text{ \AA}$  'glycolated' peak maximum, after removal of the chlorite  $14 \text{ \AA}$  line. Used for the determination of the relative smectite content.
- Illite (+ regular illite-smectite mixed layer) at  $10 \text{ \AA}$  (glycolated), to estimate relative illite content and the illite 'crystallinity' by integral breadth (see below). In some cases a removal of small pyrophyllite, **paragonite** and talc reflections

was necessary. To determine the c-lattice constant, the molybdenite corrected peak position around 10 Å was determined as exactly as possible.

- Chlorite + kaolinite - doublet at 7 Å after removal of halloysite at 7.2 - 7.5 Å if necessary; was used to determine their relative content. To separate both phases, the share of the respective mineral determined on the doublet at 3.53 - 3.58 Å (see below) was transformed to the 7 Å peak, following Biscaye (1964). The term 'kaolinite' here is used as a general expression for the kandite group or kaolin minerals.

- Molybdenite at 6.15 Å as an internal standard and for peak angle correction.

- Illite at 5 Å to approximate the 'octahedral character' by using the 5 Å/10 Å illite ratio (Esquevin, 1969). High 5 Å/10 Å values (> 0.45) normally correspond to Al-rich illites, ratios below 0.25 can be related to Fe and Mg enrichment in the octahedral layer. Biotitic illites are restricted to values below 0.1.

- Kaolinite at 3.57 - 3.58 Å and chlorite at 3.53 - 3.54 Å were identified from the slow scan diagrams mentioned above. Since only a part of our diagrams yields high peak intensities required for curve-fitting routines, the separation usually was made by doubling the respective area of the non-coinciding half of the **higher** peak. The second component was considered as the remaining area. This fast method requires symmetrical lines, which were found for the well-crystallized kandites and chlorites observed, thus leading to better results than calculations made from intensity ratios (Elverhøi and Rønningland, 1978). In the case of well-balanced proportions (K/C area ratios between 0.75 - 1.25), more accurate results were achieved using the peak doublet saddle to draw the separation line between the two phases, following the method described by Moore and Reynolds (1989, p. 302), which also requires symmetrical lines.

The determination of high angle basal spacings, which are more accurate for quantitative considerations such as 4.7 Å and 2.85 Å for chlorites, 3.35 Å for illites or all high angle smectite lines, were either not generally available for all of the samples or strongly affected by other minerals.

The relative clay mineral contents (rel.%) of smectite, illite, kaolinite, and chlorite were determined using ratios of integrated peak areas of their basal reflections, weighted by empirically estimated factors after Biscaye (1965). Accordingly the smectite 17 Å peak area is multiplied with 1, the 10 Å illite peak area with 4 and both kaolinite and chlorite shares of their 7 Å peak with 2. Due

to considerable effects of chemical and structural composition of clay minerals in relation to their spacing characters (Brindley and Brown, 1980), these weighting factors only provide a first approach to the quantity of a single phase within the clay mineral fraction. The Biscaye factors, normally applied in many marine sediment studies, in a first approximation are confirmed by an estimation of pure mineral phases with our equipment. But the factors can not be applied to rise the accuracy and inter-laboratory comparability of the results. An approach to evaluate the absolute content of a mineral phase should apply ratios computed against an internal standard (Ehrmann et al., 1992). However, ratios of peak areas of two components which indicate different source areas and transport media such as kaolinite/chlorite ratios, normally yield the best results for revealing the oceanographic conditions.

#### 3.4. 'Crystallinity' measurements

The grade of lattice ordering and the crystallite size of clay minerals, usually referred to as 'crystallinity' measurements is used to determine low temperature metamorphism of shales and slates (Frey, 1988). In young sediments possible source regions and transport paths can be traced. The measurements were made by computing the *integral breadths* (IB) of the glycolated 17 Å-smectite and 10 Å-illite peaks that means the width of the rectangle, which is of the same height and same area as the measured peak (Fig. 2). IB values are more sensitive for peak tail variations than the usually applied half height width (Krumm et al., 1991). Due to various problems of fixing the background line, IB measurements of smectite are more accurate than the v/p-index introduced by Biscaye (1965). In the case of **step scan measurements** integral breadths can be simply calculated from the integrated peak area counts multiplied with the used step size and divided by the peak intensity.

## 4. Results

### 4.1. Clay content

The clay content (Fig. 3) significantly depends on the amount of biogenic components in the sediments. High carbonate contents mainly in shallow water

depths above the CCD on ridges or in high productivity areas are normally related to low clay content. In the Polarfrontal area (around 50° S) high amounts of siliceous material like diatoms or radiolarians lead to clay contents of less than 10 % of the bulk sediment. Similar low values are encountered in areas where ice-rafting or winnowing takes place, such as along the coast-line of East Antarctica. As a result of carbonate dissolution as well as of decreasing transport energy the clay content in sediments of the abyssal basins rise to values above 50%. High clay amounts observed along the coast of Southwest Africa may be connected with river discharge or dust input. In the case of the southern deep Argentine Basin and partly of the Cape Basin, low clay content maybe ascribed to an intensive winnowing due to near-bottom currents (Ledbetter, 1986; Tucholke and Embley, 1984).

#### 4.2. Clay mineral distribution

The relative clay mineral proportions regionally vary within wide limits (Figs. 4, 5, 8 and 9). Depending on diversity of geology, climate and weathering processes of the contributing source areas, the contents for each clay mineral can change from 0 to almost 60% for chlorites, 5 to > 80% for illites, 0 to > 70% for kaolin minerals, and 0 to > 90% for smectites.

Other argillaceous minerals, such as talc, pyrophyllite, paragonite or palygorskite/sepiolite are absent or non-representative and are not taken into account. *Mixed layer components* mainly consisting of ethyleneglycol-expandable layers are often detectable as small shoulders or broad reflections between 10.5 and 14 Å. They are referred to as non-regular types of illite-smectite mixed layer components. Their appearance is strictly connected to high smectite amounts. In several locations of the Guinea and Angola Basins such mixed layer minerals are most significant, but not exceeding the amounts of the main clay mineral groups. In contrast to the observations of Biscaye (1965, p. 823), in Antarctic clays such minerals are insignificant or missing.

##### 4.2.1. Smectite

Clay fractions with more than 50 rel.% smectite are found in some spots in the Antarctic Ocean connected to volcanic environments, starting at the Pacific side of the Antarctic Peninsula and its offshore islands and stretching to the area around South Sandwich and the Southwest Indian Ridge (Fig. 4). Here the smectite distribution differs considerably from that of existing maps (Biscaye, 1965; Griffin et al., 1968). To our knowledge the smectite concentrations are the highest ever observed in the Atlantic (Weaver, 1989, p. 319). Due to the lack of samples in this area this has not been documented until now. Around young volcanos like Deception or Bouvet Island the smectite contents rise to 90 rel.%. After infrared spectroscopic measurements (pers. comm. Prof. Brockamp, University of Bremen) and (060)-peak analysis these smectites can be characterized as Fe-rich nontronites. This confirms a local non-continental origin of smectite resulting from the erosion of altered basaltic rocks **and detrital volcanic glass**, which undergo submarine weathering or **early diagenetic transformation** (Hodder et al., 1993). Other volcano-sedimentary high smectitic environments can be found on the Maud Rise and at the continental margin off Kapp Norvegia (Dronning Maud Land, East Antarctica). The latter occurrence was first described by Ehrmann et al. (1992), who identified ice-eroded altered Mesozoic basalts from Nunataks of the hinterland as a smectite source.

Smectites corresponding to such volcanogenic sedimentation are normally well-ordered. Similar observations are reported by Siever and Kastner (1976) from the Mid-Atlantic Ridge at 22°N. Connected with the main axis of the Circumantarctic Current, smectite 'crystallinity' values between South Shetland and Meteor Rise are generally below  $1.5^\circ 2\theta$  (Fig. 6a). This indicates that a considerable part of the smectite in this area is of oceanic origin. On the other hand, high 'crystallinities' but low smectite concentrations along the continental slope of East Antarctica indicate weak chemical degradation processes due to physical weathering and lack of non-metamorphic pelitic source rocks.

There are no hints for *in situ* new-formation of smectite in any of our samples. This is consistent with previous knowledge, that generally, smectite formation in Atlantic sediments is not observable (Chamley, 1989).

In the abyssal central part of the South Atlantic between 60 and 30°S as well as in the central Brazil and Angola Basins smectite concentrations are relatively high (30 - 50 rel.%). Apart from some minor inconsistencies, the smectite

distribution in these areas are in good accordance to existing maps (Griffin et al., 1968). Grain-size related segregation from land to sea may be one reason for oceanic smectite enrichment (Gibbs, 1977), especially in the Angola Basin, where high smectite concentrations are connected to poor 'crystallinities' (IB values  $> 2.0 2\theta$ , Fig. 6a). The adjacent Central African drainage area, which is characterized by high humidity and river discharge is suggested as a source region of such smectites (Van der Gaast and Janssen, 1984).

The high smectite content in the subantarctic and subtropical Atlantic could result from a combination of several factors; first, high smectite input from source areas with high amounts of Si-poor rocks (southern South America, Antarctic Peninsula, volcanics); second, relative decrease of non-smectitic material with increasing distance from the source, which is controlled by grain-size; third, transport by northerly and easterly flowing bottom currents. The latter process seems to influence the western part of the South Atlantic between Rio Grande Rise and Romanche Fracture Zone. Reflected by the 30 rel.%-isoline the zone of relative high smectite amounts here shifts from 30°S up to the equator (Fig. 4). Because of low smectite concentration at the adjacent Brazilian shelf as well as at the Mid Atlantic Ridge, [a clay mineral transport from southerly sources here can be assume.](#)

#### 4.2.2. Illite

From north to south the contour map of illite concentrations (Fig. 5) in the South Atlantic can be subdivided into five major zones:

- (1) an equatorial minimum area, **with** two **minima** of less than 10 rel.% along the Brazilian and West African shelf;
- (2) a temperate high illite region between 20°W and 20°E with values between 40 and 70 rel.%, enclosed are the Mid Atlantic Ridge, the Walvis Ridge and the northern Cape Basin;
- (3) a large region of moderate illite contents between 30 and 40 rel.% within the central and subpolar parts of the South Atlantic, the latter are characterized by some **minima** of 5 - 20 rel.% and good illite 'crystallinities' (Fig. 6b);
- (4) a zone of high illite amounts (50-65 rel.%) within the Weddell Sea and near the Ronne/Filchner Shelf (West Antarctica);

(5) a zone of extremely high illitic clays along the East Antarctic continental shelf and at the adjacent deep sea with values between 65 and > 80 rel.%.

(1) Illite minerals are rare in the equatorial South Atlantic especially at the Brazilian and Central and West-African coasts, which are related to the well-known high kaolinitic region, receiving soil material from humid tropical regions drained by rivers and/or to input of eolian dust from deserts ([references see in introduction](#)). The octahedral character of corresponding illites in this area normally appears as Al-rich (Fig. 7a). Although sediments with similar illites occur in the western part of the South Atlantic south of 50°S, the 5 Å/10 Å ratios are highest in low latitudes, partly exceeding 0.60 (Fig. 7a). These chemically more stable illites are probably derived from residual clays, which survived warm and humid weathering processes in the source regions.

Low-ordered illites in deep accumulation areas of the Angola and Guinea Basins are related to illite/smectite mixed layer minerals containing ethylene glycol expandable components, [providing small shifts of the 10 Å peak position shown in Fig. 7b](#). However, in the main parts of the Guinea Basin illites are well-ordered (IB values between 0.3 and 0.4° 2 $\theta$ ., Fig. 6b), whereas in the Brazil Basin and near the coasts structurally degraded illites prevail (> 0.5° 2 $\theta$ .). The reason for this is difficult to explain. Well-ordered clay minerals normally appear in regions with little chemical degradation. Dust input from the arid areas of Northwest Africa may serve as possible source of well ordered illites in the Guinea Basin (Gingele, 1992).

(2) The second region is shaped like a northerly clockwise rotated lobe, covering large areas of the subtropical eastern part of the South Atlantic (Fig. 5). Starting at the South African shelf and continental slope, high percentages of illite are observed, which confirms former investigations (Bornhold, 1973; Bornhold and Summerhayes, 1977). Due to the landward increase up to 70 rel.%, an illite source from the Namibian deserts is obvious. Part of the material may be derived from South African soils, which are known to be rich in illite (Van der Merwe, 1966). Due to the increasing input of smectite by rivers (e.g. Kunene) north of 20°S illite contents rapidly drop below 30 rel.% (Bremner and Willis, 1993).

(3) The third zone covers the western and central part of the South Atlantic including the Antarctic Circumpolar Current region down to 60°S. Apart of some minor differences, this zone is concordant with the large smectite-rich region mentioned above. For that reason, the conditions for the distribution of illite and smectite should be very similar. In contrast to previous illite concentration maps last compiled by Windom (1976), at the Brazilian and Argentinian continental shelf, we do not see any continentally derived illite lobes (concentrations above 50% illite) in our data, probably depending on our sample availability. Several profiles from the deep sea to the shelf more likely indicate an illite decrease in this direction, especially at 20°S.

In subpolar regions some of the illite **minima** are strongly correlated to the volcano-sedimentary patches of smectite maxima, which are discussed above. Near volcanic source areas like Bouvet Island illite even disappears completely. Illites within the circum Antarctic area normally show c-lattice constants below 9.98 Å (Fig. 7b) and appear as highly 'muscovitic'. Most of illites situated in zone 3 are well-ordered. The IB values are usually below  $0.5^\circ 2\theta$  (Fig. 6b). In eastern parts of the South Atlantic Polarfrontal area particularly well-crystallized illites are encountered. 10Å integral breadths of less than  $0.4^\circ 2\theta$  are observed in the area south of the Polar Front and related to Al-rich illites. Similar results are reported from the Polar Frontal Zone of the Eastern Indian Ocean by Moriarty (1977).

The source region for such illites can easily be traced to granitoid and low metamorphic andean rocks in the southern part of South America and West Antarctica. Some components may be derived from the Pacific coast of Antarctica via the Drake Passage.

(4) In the northern and western Weddell Sea south of the Antarctic Circumpolar Current (ACC) the illite concentrations rise from < 40 rel.% to > 50 rel.% (Fig. 5). This sudden increase more or less coincides with the ACC/Weddell gyre boundary, outlining an important clay facies borderline within the Antarctic Ocean, which is also reflected by kaolinite and chlorite concentrations. In general, the 'crystallinities' as well as the 5 Å/10 Å ratios of illites in Weddell Sea sediments decrease slightly. Only sediments supplied from the Filchner Ice Shelf and from Berkner Island carry well-ordered and Al-rich illites. Low metamorphic sedimentary and felsic igneous rocks of West Antarctica are

probably the main illite source. Similar to the volcanic areas in the north, the smectite-rich Maud Rise region appears as an illite-depleted anomaly.

(5) The most striking feature of the contour maps describing all illite parameters (Figs. 5, 6b, 7a and 7b) is apparent along the continental margin off East Antarctica. In this area illite concentrations are extremely high increasing to values above 70 rel.%, in samples near the Antarctic coast even up to 85 rel.%. In the eastern part (Lazarev and Rijser Larsen Sea) the 70 rel.%-isoline is parallel to the 4000 m water depth contour line. In westerly direction along the continental rise the isolines follow the main oceanographic current patterns, i.e. the East Antarctic Coastal Current as a part of the Weddell Gyre. The westward extension of the 70 rel.% isoline is attributed to the advection of high illitic clays from the East more than 30 degree in longitude to the West.

At the western edge of the East Antarctic Shield, off the Rijser-Larsen and Jelbert Ice Shelf illite concentrations decrease down to 40 rel.% reflecting a different hinterland geology. Further south off the Luitpold Coast illite contents rise to 80 rel.% once again (Ehrmann et al., 1992).

Generally high IB values of more than  $0.8^\circ 2\theta$  indicate low 'crystallinities' in this region (Fig. 6b). Particular low  $5 \text{ \AA}/10 \text{ \AA}$  ratios ( $< 0,1$ ) and  $d(001)$ -values exceeding  $10.0 \text{ \AA}$  (in parts more than  $10.1 \text{ \AA}$ !) are typical for illites of Fe(+Mg)-rich octahedral character, which are related to clay mineral assemblages containing high amounts of biotite-derived components (Fig. 7b). Some (060) reflection measurements made on texture-free preparations confirm the occurrence of trioctahedral illites, but due to coinciding chlorite and quartz lines it is difficult to estimate their amount. We never observed a lack of dioctahedral (060)-reflections in any sample.

The enrichment of such detritic Fe-(Mg)-rich illites, which are uncommon in the marine environment can be ascribed to the dominance of biotite-bearing highly metamorphic rocks in the East Antarctic craton. Under non-glacigene weathering processes such micas normally suffer a complete degradation and rapid transformation to other clay minerals like vermiculite, smectite, and hydrobiotite. Consequently they disappear before reaching the marine system. Since in glacigene regimes physical degradation like grain diminution

predominates, low-ordered 'biotite-like' illites preserve their chemical and structural properties and are supplied to the ocean.

#### 4.2.3. Kaolinite

The distribution of tropical continentally derived kaolin minerals north of 30°S exhibits the strongest latitudinal control of all of the clay mineral groups discussed (Fig. 8), which is apart from some minor deviations well-documented by previous authors (Biscaye, 1965; Windom et al., 1975). South of 30°S latitude a slight asymmetry is developed by the 10 rel.% line, which shifts more than 10° further south in the Cape Basin compared to the Argentine Basin.

South of 50°S the kaolinite content plotted in previous world-wide maps remains very low, mostly below 5 rel.% (Griffin et al., 1968). According to our samples from the Antarctic Ocean, that **minima** is restricted to the circum Antarctic region between 50 and 60°S and related to high smectite and chlorite concentrations.

In the Weddell Sea **and Enderby Basin** the kaolinite content increases slightly to values between 5 and 10 rel.% south of 60°S. Some kaolin-rich sediments known from the Ronne and Filchner Ice Shelf hinterland, especially from Berkner Island may be responsible for that enrichment (**Fütterer and Melles, 1990**, Ehrmann et al., 1992) by supplying "fossil" kaolinite to the main parts of the Weddell Sea. East of Maud Rise the kaolinite contents rise to more than 10 rel.%. These are exactly the same amounts which are found in sediments of the temperate seas of the South Atlantic! No connection of this kaolinite enrichment zone to possible East Antarctic sedimentary source rocks could be drawn (Fig. 8). In easterly direction the next kaolin-bearing rocks are found out of the investigation area in the Amery formation at about 60°E (ref. in Ehrmann et al., **1991**). As a further possible source we assume locally eroded kaolinite-bearing Tertiary sediments **recovered** from submarine ridges (Maud Rise, Astrid-, or Gunnerus Rigde). According to Robert and Maillot (1990) and Robert and Kennett (1992) Paleogene sediments of the Maud Rise contain up to 20% kaolinite.

Since Fe-illites increase strongly close to the East Antarctic margin (Fig. 5 and 7b), kaolinite concentrations decrease to values lower than 5 rel.%. As a consequence of missing source rocks kaolin minerals can disappear completely on the shelf.

#### 4.2.4. Chlorite

In relation to the kaolinite contour map presented above, the chlorite distribution (Fig. 9) appears as an inverted copy (Rateev et al., 1969). Chlorites are depleted in two distinct minimum zones of less than 5 rel.%. Both correspond to kaolinite maxima.

The first zone is confined to low latitudes along the coasts off Brazil and West Africa and also covers large parts of the Guinea and Angola Basins. Chlorites are destroyed under the warm and humid climates of the adjacent tropical source area and do not reach the ocean in significant amounts. Further south in the Southern Angola Basin and off the Namib desert, chlorite contents rise beyond 10 rel.%. Along the South African coast and in main parts of the eastern Cape Basin chlorite concentration remains lower than 10 rel.%.

The second previously unknown region of particularly low chlorite amounts is found east of the Maud Rise, where clay mineral assemblages are dominated by Fe-Illite in the south and minor kaolinite in the north. Similar to high illite contents (Fig. 5), the low chlorite **environment** can be traced along the eastern boundary of the Weddell Sea to 30°W, where **it is** replaced by chlorite-rich sediments derived from the Filchner Ice Shelf. Higher chlorite contents are locally observed on the narrow shelf along the western part of East Antarctica.

The most striking element of chlorite distribution is the distinct meridional maximum at the Subantarctic and Polarfront regions, which shows concentrations of more than 20 rel.% stretching all along the southern Atlantic up to Meteor Rise and east of the Greenwich meridian (Fig. 9). The orientation of that zone clearly indicates that chlorite-bearing source areas are found at the Pacific realm of southernmost America and of the Antarctic Peninsula. Some chlorite may be derived from South Georgia and South Orkney Island were the

values even exceed 40 rel.%. Chlorite concentrations up to 60 % are observed in the western Brainsfield strait (Yoon et al., 1992).

In the Argentine Basin a branch of high chlorite concentrations is developed (Biscaye, 1965), which is associated with the continental contour current and cold water flow of Lower Circumantarctic Deep Water through the Vema Channel (Jones and Johnson, 1984).

#### 4.3. *Kaolinite/Chlorite ratio*

The distribution of clay mineral provinces is best illustrated if contents of two minerals of **different** origin are plotted as a ratio. Therefore, in plots of kaolinite/chlorite ratios (Fig. 10) zonal factors of single mineral distributions appear amplified. In contrast to previous maps working with that ratio, a symmetrical latitudinal zonation (Weaver, 1989) is restricted to the non-Antarctic part of the South Atlantic. South of 60°S kaolinite concentrations increase.

If oceanographic current systems monitor the clay mineral transport and their sedimentation, kaolinite/chlorite ratios can be used as an indicator of deep water mass influence. Plotting all of the kaolinite/chlorite values available between 10°W and 20°E (the area of our best sample availability, covering the whole water column) into a latitude **vs.** water depth diagram (Fig. 11a) a zonal clay mineral layering within the South Atlantic water column between 30 and 50°S appears. Therefore, a predominant advection of relative kaolinite rich material within the southward flowing North Atlantic Deep Water mass up to 50°S is evident. The Circumantarctic Deep Water as a counterpart carries chlorite-rich sediment from the west, causing chlorites to culminate at the Polarfrontal-Zone (50 - 60°S), which in turn results in a mixing and successive reducing of the kaolinite signal. Therefore low-latitudinal kaolinite bearing suspensions presently do not reach the Antarctic margin. Following the thermohaline layering (Fig. 11b), the chlorite signal remains detectable near the bottom over more than 15° in latitude into northerly direction. Although only a few samples are available, the same is assumed to work at shallower water depths. A relation between chlorite content and the spatial distribution of Antarctic Intermediate

Water (AAIW) is assumed. North of 40°S an additional input of chlorite from South Africa is documented (black dots in Fig. 11a).

The clay mineral distribution around 30 - 50°S causes some maxima and minima shown in Fig. 10. A similar kaolinite and chlorite distribution driven by deep water masses is developed in the Vema Channel region (Chamley, 1975; Jones, 1984). Such depth related clay mineral distributions in abyssal regions can only develop if clay material transport is advective (Jones, 1984) and if suspension loads increase with water depth.

## 5. Discussion: Clay mineral facies provinces

The distribution of all clay mineral assemblages shown in the previous maps and compiled from literature data were summarized in Fig.13. A subdivision into ten principal clay mineral provinces is made, each characterized by similar clay mineral composition (Fig. 12) resulting from comparable climate and geology of the involved source areas and by unique oceanographic conditions (Table 1). Most of the borders between the zones are very smooth, so that an exact construction of transitions is difficult. Furthermore, near the adjacent continents the clay mineral distribution is usually more complex than displayed in Fig. 13.

In the equatorial province a subdivision into a central 'oceanic' and two lateral 'continental' subprovinces can be made. The *lateral Equatorial subprovinces* describe regions with more than 50 rel.% kaolinite which are consistent with areas in which chlorite and to some extent Al-rich illite contents drop below 5 rel.%, and 20 rel.%, respectively. Kaolinites are formed under lateritic weathering regimes in the adjacent hinterland and supplied to the near-continent environment by fluvial or aerial input. In lateritic soils gibbsite is an essential component and is observed in all of our clay fractions found in this subprovince (Van der Gaast and Jansen, 1984).

As already mentioned by Biscaye (1965), the western Brazilian part is characterized by primary river-derived clayey material, which is transported latitudinally (and partly resuspended) along the small shelf of South America by the Brazil current, leading to a southern kaolinite lobe near Rio de Janeiro.

The eastern African lateral Equatorial subprovince covers the Guinea Basin and the northern Angola Basin. Here, river-derived clayey material drained from Central African soils is mixed with wind-borne dust transported by NE and SE-trades from the Sahel Zone and Southwest Africa (Gingele, 1992). Indicated by a few samples the kaolin-rich zone west of the Greenwich Meridian extends south to 20°S, which may be related to a possible latitudinal advection of dust components within the North Atlantic Deep Water. Similar structures showing a reversion of transport paths from northwest (caused by wind) to south (driven by oceanography) are found in the smectite-rich Angola Basin province and the illite-rich Cape-Walvis Ridge province, which are discussed later.

In the *Central Equatorial subprovince* kaolinite contents are higher than for any other single clay mineral, usually above 30 rel.%, but they do not exceed 50%. A mixed clay mineral assemblage deposited under abyssal conditions with different source areas is assumed. Some of the clayey material found in this province (e.g. illites) may be imported by North Atlantic Deep Water from higher latitudes, thus diluting the kaolinite signal.

The *Central Angola Basin province* is characterized by high contents of low ordered smectite (> 30 rel.%), which is formed under highly hydrolytic conditions, supplied by Southwest-African rivers like the Kunene and carried to the north by the Benguela Coastal Current (Gingele, 1992, Bremner and Willis, 1993). In this zone kaolinite successively increases from south to north from 20 to 50%. The SE-trades may contribute some of this material to the central Angola Basin. However, smectite contents in aerosols are highly variable and depend on the sampling technique (Johnson, 1976). The rotated shape of the western part of this province may be formed by southward flowing North Atlantic Deep Water (NADW).

The illite rich zone of the *Cape-Walvis Ridge province* follows to the south, outlined by the 40 rel.% isoline (Fig. 5) and partly by the decrease of the smectite content below 30 rel.% (Fig. 4). Both kaolinite and chlorite contents hardly reach 20 rel.%. The kaolinite/chlorite ratio normally varies between 1 and 3. This province coincides with the illite zone (2) of Ch. 4.2.2. **The westward and later northward extension of this zone does not show any direct relation to the predominant northwesterly directed wind systems or to upper**

level oceanography. A complex interaction of illite input by trade winds, transport by surface and intermediate water masses and dilution by kaolinite in the Guinea and Northern Angola Basin is assumed. The advection of illites into the northern Cape Basin seems to be supported by westerly flowing bottom currents contouring the Walvis Ridge (Tucholke and Embley, 1984). A possible input of cold bottom water from the Cape to the Angola Basin at the Walvis Kom (Shannon and Chapman, 1991) may explain the continuation of the illite rich zone in the southwestern Angola Basin. Some illite may be contributed by the submarine erosion of the Walvis Ridge itself.

The *Central South Atlantic province* covers large parts of the Argentine and Brazil Basins, the Southern Cape Basin and the Agulhas Basin. This zone is characterized by illite and smectite concentrations of more than 30 rel.%. Here, a layering of kaolinite and chlorite distribution due to the thermohaline deep water hydrography of the South Atlantic is proved to be well-developed at least in the Vema Channel region and in the Agulhas Basin (Ch. 4.3.). Advection of clayey material from low and high latitudes by deep water masses results in clay mineral assemblages outlined by the **distribution** of the respective water masses. The asymmetric shape of the province is explained by stronger southward advection of low latitude material derived from Africa in the eastern basins combined with the stronger northward transport of high latitude clays in the cold deep water masses, which prevail near the bottom in the western basins.

The *Antarctic Circumpolar province* is outlined by the 20 rel.% isoline of the chlorite content and by kaolinite lows of less than 5 rel.%. Illite minerals are normally well-crystallized. Such matter is derived from low metamorphic rocks like greenschists or meta-greywackes mainly found in the Andean chain on the Pacific side of the Antarctic Peninsula and southernmost America. Transport by the Antarctic Circumpolar Current, which is amplified in the Drake Passage is the main driving force. Primarily, most of the clayey material is advected in suspension within the Circumantarctic Deep Water (CDW) body. Most chlorite minerals on the Greenwich schematic profile are found in water depths between 500 and 4500 m **and are related to** CDW (Fig. 11). As an effect of Weddell Sea Deep Water inflow below **4500 m** kaolinite/chlorite values appear slightly decreased. **Secondary**, transport by sediment-laden icebergs and some dust import may influence the modern clay composition. Since all the material is

derived from common regions of denudation, no differentiation of **these** transport processes can be detected from clay mineralogy.

In the *Weddell Sea province* a mixed clay mineral assemblage occurs dominated by illite (about 50 rel.%) of moderate 'crystallinity' and medium 5Å/10Å values. Chlorite contents drop below 20 rel.%, kaolinite varies between 5 and 10 rel.% and smectite ranges from 10 to 30 rel.%. This clay mineral ensemble sharply appears south of the **ACC/Weddell Gyre boundary**. An origin from West Antarctica is most likely (**Ch. 4.2.2**). Although some clayey material within this area may be contributed by ice rafting, most is related to sediments transported into the marine environment by ice shelves (Fütterer and Melles, 1990; Ehrmann et al., 1992). The material is supplied by surrounding glaciers and released to the ocean by melting near the grounding line of the ice shelves. The subsequent transfer of fine illite-rich suspensions to the deep-sea is ascribed to cold thermohaline bottom currents, which generates the Weddell Sea Bottom Water, and to turbidity currents (Kuhn and Weber, 1993). Due to oceanography characterized by the cyclonic Weddell Gyre a bottom and contour current transport of clayey mud is active in the Weddell Abyssal Plain (Pudsey, 1993). The shape of the Central Weddell Sea province is in remarkably good accordance to deep and intermediate layered geostrophical and thermohaline circulation patterns stretching to the northwestern Enderby Abyssal Plain up to 30°E, which were recently compiled by Orsi et al. (1993).

The *East Antarctic province* can be subdivided into a **southern part** which is characterized by more than 70 rel.% 'biotitic' illite plus little or no kaolinite, and a **northern part** in which kaolinite exceeds 10 rel.%. Chlorite contents are only minor (< 10 rel.%) and smectite concentrations remain mostly below 20 rel.%. The **northern part** is mainly developed at the southern Enderby Abyssal Plain, related to **westward flowing kaolinite-bearing suspensions**. The boundary line between West Antarctic to East Antarctic clay **composition** appears as a sharp **NE - SW striking** borderline near the Maud Rise, tracing the backflow of the Weddell Gyre to the southwest (Orsi et al., 1993).

The illite distribution (Fig. 5) shows that the **southern part** of the East Antarctic province (Rijser Larsen and Lazarev Seas) is strongly influenced by the high-grade metamorphic rocks found in Dronning Maud Land. The westerly transport of biotite-bearing suspensions into the Weddell Sea contouring the continental

margin is mainly attributed to the East Antarctic Coastal Current and the southwesterly flow of CDW and WSDW within the Weddell Gyre.

## 6. Conclusions

Previous knowledge has been confirmed that most of the clay minerals found in the South Atlantic are of continental origin. Local enrichments of nontronites found around denudated submarine basaltic rocks are the only considerably exception. This is the first occurrence described in the South Atlantic. Nevertheless, the bulk of (montmorillonite) smectite in the abyssal plains is terrigenous. However, it is difficult to prove to what extent a mixing of smectite of different genesis takes place. Evidence for a detrital source is shown in the slight asymmetrical distribution, where smectite is more restricted to the western basins of the central South Atlantic (Fig. 4), indicating a South American and West Antarctic origin.

Clay mineral assemblages of deep-sea sediments do not indicate only one single source area and transport path. Nevertheless, we tried to demonstrate, that main transport and resuspension of clay detritus is driven by oceanographic currents especially within deep water regimes. Deep and bottom water masses carry fine-grained material imported to the deep marine environment by wind, river, ice, turbidity and thermohaline currents. Thus, deep water transport additionally causes a distinct extension of deposition provinces of the source areas.

Direct input by *rivers* is restricted to the shelves of West-Africa and South America. A considerable amount of *aerosol* material can be expected in the northeastern abyssal plains, derived from African deserts. *Ice rafted* clay detritus contributes to the clay mineral assemblages of the Antarctic shelves but is a minor source for the deep sea sediments. A direct input by *turbidity currents* is hard to determine by clay mineral distribution. In abyssal plains the clay distribution appears to be highly superimposed by *contour current* resuspension. Although our sample distribution is incomplete, and the clay mineral zones in most cases are configured parallel to the steep slopes of Antarctica and South America, they do not show lobes or branches into deep-sea areas, which would be expected from a higher influence of turbidity current action. Along the South American margin such lobes were mapped by Griffin et al. (1968).

As a result, we were able to show, that the main source regions for abyssal South Atlantic clayey material are named as follows in order of their importance:

- The *Andean chain of southernmost America and the Antarctic Peninsula*. yields clayey material predominantly derived from glacial erosion, which enters the entire Subantarctic region and the western border of the Argentine Basin. Chlorite-rich clay detritus as a typical tracer may additionally be contributed from the Pacific margin of Antarctica as well as from rivers of South America. The main abyssal transport process is driven by oceanography, primary the Antarctic Circumpolar Current. Further north, on the way from the Argentine Basin to the Brazil Basin as well as in the southern Cape Basin the main advection of clayey material takes place within southern component waters (mainly LCDW). In the Cape Basin chlorite and smectite derived from Africa are consecutively diluted with clayey material transported by the North Atlantic Deep Water (NADW). Smectites found in the Brazil Basin appear to travel the longest distances.

- Material from *West- and Southwest Africa*, which dominates in sediments within the Guinea Basin, Angola Basin, and northern Cape Basin, originates from distinct regions of kaolinite, smectite, and illite dominance. These regions are related to the weathering regime, climate and type of soil formation. The transport to the deep sea results from a complex interaction of river and wind input and distribution by ocean currents. Further west, the role of deep current systems seems to be dominant, mainly represented by North Atlantic Deep Water. A part of the clayey detritus carried in the NADW may derived from North African deserts. Dust loads of the NE-trades rain out in the innertropical convergence zone (ITCZ) (Pokras and Mix, 1985), where they are introduced to deeper waters. A mixing of such clay mineral assemblages with polar and subpolar components is indicated in the Agulhas and southern Cape Basin by a **depth related** clay mineral layering within the deep water column.

- *West-Antarctica* is the source area of most of the clayey material found in the Weddell Sea. Illite and smectite rich material derived from the catchment areas of the Filcher- and Ronne-Iceshelves enters the deep sea, driven by inflow of new-formed cold bottom water and by the Weddell Gyre.

- The influx clay minerals from *East-Antarctica* is detectable in an area covering the southern Enderby Abyssal Plain, Lazarev and Riisser Larsen Sea, which is outlined by Fe-Mg-rich illite and kaolinite.

- Material from *NE-Brazil* can be found only on the adjacent shelf and near the continental margin. Its contribution to the Brazil- and Argentine Basins appears to be relatively low.

### **Acknowledgements**

We thank the *Deutsche Forschungsgemeinschaft*, Bonn for supporting clay mineral investigations on Antarctic sediments, project Ku 683/2. A considerable amount of samples were prepared by H. Rhodes and R. Fröhlking. For critical reviews of the manuscript we are grateful to Dr. W. Ehrmann, Bremerhaven and M. Tintelnot, Senckenberg Institut, Wilhelmshaven, and ..... This is publication 82 of Special Research Project SFB 261 and contribution No. xxx. of the Alfred Wegener Institute for Polar and Marine Research, Bremerhaven

### **References**

Anderson, J.B., Kurtz, D.D., Domack, E.W. and Balshaw, K.M., 1980a. Glacial and glacial marine sediments of the Antarctic continental shelf. *J. Geol.*, 88: 399-414.

Anderson, J.B., Domack, E.W. and Kurtz, D.D., 1980b. Observations of sediment-laden icebergs in Antarctic waters: Implication to glacial erosion and transport. *J. Glaciol.*, 25: 387-396.

Aston, S.R., Chester, R., Johnson, L.R. and Padgham, R.C., 1973. Eolian dust from the lower atmosphere of the eastern Atlantic and Indian Ocean, China Sea and Sea of Japan. *Mar. Geol.*, 14: 15-28.

Baretto, L.A., Milliman, J.D., Amaral, C.A.B. and Francosconi, O., 1975. Northern Brazil. In: J.D. Millimann and C.P. Summerhayes (Editors), Upper Continental Margin Sedimentation off Brazil. *Contrib. Sediment.*, 4, pp. 11-43.

Behairy, A.K., Chester, R., Griffiths, A.J., Johnson, L.R. and Stoner, J.H., 1975. The clay mineralogy of particulate material from some surface seawaters of the eastern Atlantic Ocean. *Mar. Geol.*, 18: M45-M56.

Biscaye, P.E., 1964. Distinction between kaolinite and chlorite in recent sediments by X-ray diffraction. *Am. Miner.*, 49: 1281-1289.

Biscaye, P.E., 1965. Mineralogy and sedimentation of recent deep-sea clay in the Atlantic Ocean and adjacent seas and oceans. *Geol. Soc. Am. Bull.*, 76: 803-832.

Biscaye, P.E. and Eittreim, S.L., 1977. Suspended particulate loads and transports in the nepheloid layer of the abyssal Atlantic Ocean. *Mar. Geol.*, 23: 155-172.

Bornhold, B.D. (Editor), 1973. Late Quaternary sedimentation in the eastern Angola Basin. Woods Hole Techn. Rep. WHOI 73-80, Massachusetts, W.H.I.O., 213 pp.

Bornhold, B.D. and Summerhayes, C.P., 1977. Scour and deposition at the foot of the Walvis Ridge in the northernmost Cape Basin, South Atlantic. *Deep-Sea Res.*, 24: 743-752.

Bremner, J.M. and Willis, J.P., 1993. Mineralogy and geochemistry of the clay fraction of sediments from the Namibian continental margin and the adjacent hinterland. *Mar. Geol.*, 115: 85-116.

Brindley, G.W. and Brown, G. (Editors), 1980. *Crystal Structures of Clay Minerals and Their X-ray Identification*. Miner. Soc. Monogr., 5, London, 495 pp.

Chamley, H., 1975. Influence des courants profonds au large du Brésil sur la sédimentation argileuse récente. 9ème Cong. Int. Sédimentol. (Nice) 8: 13-17.

Chamley, H. (Editor), 1989. *Clay Sedimentology*. Springer-Verlag Berlin-Heidelberg-New York, 623 pp.

Chester, R., Elderfield, H., Griffin, J.J., Johnson, L.R. and Padgham, R.C., 1972. Eolian dust along the eastern margins of the Atlantic Ocean. *Mar. Geol.*, 13: 91-105.

Drever, J.I., 1973. The preparation of oriented clay mineral specimens for X-ray diffraction analysis by a filter-membrane peel technique. *Am. Miner.*, 58: 553-554.

Ehrmann, W.U., Grobe, H. and Fütterer, D.K., 1991. Late Miocene to Holocene glacial history of East Antarctica revealed by sediments from Sites 745 and 746. *Proc. ODP, Sci. Results*, 119: 239-260.

Ehrmann, W.U., Melles, M., Kuhn, G. and Grobe, H., 1992. Significance of clay mineral assemblages in the Antarctic Ocean. *Mar. Geol.*, 107: 249-273.

Eisma, D., Kalf, J. and Van der Gaast, S.J., 1978. Suspended matter in the Zaire estuary and the adjacent Atlantic ocean. *Netherl. J. Sea Res.*, 12: 382-406.

Elverhøi, A. and Roaldset, E., 1983. Glaciomarine sediments and suspended particulate matter, Weddell Sea Shelf, Antarctica. *Polar Res.*, 1: 1-21.

Elverhøi, A. and Rønningsland, T.M., 1978. Semiquantitative calculation of the relative amounts of kaolinite and chlorite by X-ray diffraction. *Mar. Geol.*, 27: M19-M23.

Esquevin, J., 1969. Influence de la composition chimique des illites sur le cristallinité. *Bull. Centre Rech. Pau. S.N.P.A.*, 3: 147-154.

Frey, M., 1987. Very low-grade metamorphism of clastic sedimentary rocks. In: M. Frey (Editor), *Low Temperature Metamorphism*. Blackie, Glasgow & London, pp. 9-58.

Fütterer, D.K. and Melles, M., 1990. Sediment patterns in the southern Weddell Sea: Filchner Shelf and Filchner Depression. In: U. Bleil and J. Thiede

(Editors), Geological History of Polar Oceans: Arctic versus Antarctic. (NATO/ASI Ser. C, 308.) Kluwer, Dordrecht, pp. 381-401.

Gibbs, R.J., 1977. Clay mineral segregation in the marine environment. *J. Sediment. Petrol.*, 47: 237-243.

Gingele, F., 1992. Zur klimaabhängigen Bildung biogener und terrigener Sedimente und ihrer Veränderung durch die Frühdiagenese im zentralen und östlichen Südatlantik. *Berichte FB Geowissensch. Uni Bremen*, 26: pp. 202.

Griffin, J.J., Windom, H. and Goldberg, E.D., 1968. The distribution of clay minerals in the World Ocean. *Deep-Sea Res.*, 15: 433-459.

Grobe, H., 1986. Sedimentation processes on the antarctic continental margin at Kapp Norvegia during the Late Pleistocene., *Geol. Rundsch.*, 75: 97-104.

Grobe, H., Fütterer, D.K., Hubberten, H.W., Kuhn, G. and Mackensen, A., 1993. Zur Entwicklung der spätquartären Sedimentfazies im Südpolarmeer. *Zeitschr. dt. geol. Ges.*, 144: 330-351.

Hodder, A.P.W., Naish, T.R. and Nelson, C.S., 1993. A two-stage model for the formation of smectite from detrital volcanic glass under shallow-marine conditions. *Mar. Geol.*, 109: 279-285.

Johnson, L.R., 1976. Particle-size fractionation of eolian dusts during transport and sampling. *Mar. Geol.*, 21: M17-M21.

Jones, G.A., 1984. Advective transport of clay minerals in the region of the Rio Grande Rise. *Mar. Geol.*, 58: 187-212.

Jones, G.A. and Johnson, D.A., 1984. Displaced Antarctic diatoms in Vema Channel sediments: Late Pleistocene/Holocene fluctuations in AABW flow. *Mar. Geol.*, 58: 165-186.

Krumm, S. and Buggisch, W., 1991. Sample preparation effects on illite crystallinity measurements: grain size gradation and particle orientation. *J. metam. Geol.*, 9: 671-677.

Kuhn, G. and Weber, M., 1993. Acoustical characterization of sediments by Parasound and 3.5 kHz systems: Related sedimentary processes on the southeastern Weddell Sea continental slope, Antarctica. *Mar. Geol.*, 113: 201-217.

Kumai, M., 1976. Identification of nuclei and concentrations of chemical species in snow crystals sampled at the South Pole. *J. Atmos. Sci.*, 33: 833-841.

Ledbetter, M.T., 1986. Bottom-current pathways in the Argentine Basin revealed by mean silt particle size. *Nature*, 321: 423-425.

McManus, D., 1991. Suggestions for authors whose manuscripts include quantitative clay mineral analysis by X-ray diffraction. *Mar. Geol.*, 98: 1-5.

Moore, D.M. and Reynolds Jr., R.C. (Editors), 1989. *X-Ray Diffraction and the Identification and Analysis of Clay Minerals*. Oxford University Press, pp. 332.

Moriarty, K.C., 1977. Clay minerals in Southeast Indian Ocean sediments, transport mechanisms and depositional environments. *Mar. Geol.*, 25: 149-174.

Orsi, A.H., Nowlin Jr., W.D. and Whitworth III, T., 1993. On the circulation and stratification of the Weddell Gyre. *Deep-Sea Res. I*, 40: 169-203.

Peterson, R.G. and Whitworth III, T., 1989. The subantarctic and polar fronts in relation to deep water masses through the southwestern Atlantic. *J. Geophys. Res.*, 94, C8: 10817-10838.

Pokras, E.M. and Mix, A.C., 1985. Eolian evidence for spatial variability of Late Quaternary climates in tropical Africa. *Quat. Res.*, 24: 137-149.

Prospero, J.M., 1981. Arid regions as sources of mineral aerosols in the marine environment. In: T.K. Pewe (Editor), *Desert Dust: Origin, Characteristics, and Effect of Man*, *Geol. Soc. Amer. Spec. Paper*, 186: pp. 71-86.

Pudsey, C.J., 1992. Late Quaternary changes in Antarctic Bottom Water velocity inferred from sediment grain size in the northern Weddell Sea. *Mar. Geol.*, 107: 9-33.

Quakernaat, J., 1970. Direct diffractometric quantitative analysis of synthetic clay mineral mixtures with molybdenite as orientation-indicator. *J. Sediment. Petrol.*, 40: 506-513.

Rateev, M.A., Gorgunove, Z.N., Lisitzyn, A.P. and Nosov, G.L., 1969. The distribution of clay minerals in the oceans. *Sedimentology*, 13: 21-43.

Reid, J.L., 1989. On the total geostrophic circulation of the South Atlantic Ocean: Flow patterns, tracers, and transports. *Progr. Oceanog.*, 23: 149-244.

Robert, C. and Kennett, J.P., 1992. Paleocene and Eocene kaolinite distribution in the South Atlantic and Southern Ocean: Antarctic climatic and paleoceanographic implications. *Mar. Geol.*, 103: 99-110.

Robert, C. and Maillot, H., 1990. Paleoenvironments in the Weddell Sea area and Antarctic climates, as deduced from clay mineral associations and geochemical data, ODP Leg 113. *Proc. ODP, Sci. Results*, 113: 51-70.

Shannon, L.V. and Chapman, P., 1991. Evidence of Antarctic Bottom Water in the Angola Basin at 32°S. *Deep-Sea Res.*, 38: 1299-1304.

Siever, R. and Kastner, M., 1967. Mineralogy and petrology of some Mid-Atlantic Ridge sediments. *J. Mar. Res.*, 25: 263-278.

Tucholke, B.E. and Embley, R.W., 1984. Cenozoic regional erosion of the abyssal sea floor off South Afrika. In: J.S. Schlee (Editor), *Interregional unconformities and hydrocarbon accumulation*. U. S. Geol. Surv., Woods Hole, MA, United-States. AAPG-Mem., 36: pp. 145-164

Van der Gaast, S.J. and Jansen, J.H.F., 1984. Mineralogy, opal, and manganese of middle and late Quaternary sediments of the Zaire (Congo) deep-sea fan: origin and climatic variation. *Neth. J. Sea Res.*, 17: 313-341.

Van der Merwe, C.R., 1966. Soil groups and subgroups of the southern Africa. *Publ. Dept. Agricult. Tech. serv.*, South Africa, 231: 1-353.

Weaver, C.E., 1989. Clays, Muds, and Shales. *Developm. Sediment.*, SEPM, 44, pp. 819.

Windom, H.L., 1976. Lithogenous material in marine Sediments. In: J.P. Riley and R. Chester (Editors), Chemical Oceanography. Academic Press, New York, London, 5: pp. 103-135.

Yoon, H.I., Hab, M.W., Park, B.K., Han, S.J. and Oh, J.K., 1992. Distribution, provenance, and dispersal pattern of clay minerals in surface sediments, Bransfield Strait, Antarctica. Geo-Mar. Letters, 12: 223-227.

## Figure Captions

Fig.1: Map of sample distribution, comprising multicorer, minicorer and large box corer sites.

Fig. 2: Representative diffraction profile of ethylene-glycolated smectite rich clay (CoK $\alpha$ ). Integral breadths of 17 Å smectite and 10 Å illite reflections are used to estimate their degree of ordering ('crystallinity'). Detailed explanations are given in the methods section.

Fig. 3: Percentage of clay content (< 2  $\mu$ m).

Fig. 4: Smectite distribution, plotted as percentage of weighted 17Å peak area.

Fig. 5: Illite distribution, plotted as percentage of weighted 10Å peak area.

Fig. 6 (a and b): Distribution of smectite (a) and illite (b) 'crystallinity', computed as integral breadths (compare Fig. 2).

Fig. 7 (a and b): Distribution of 5 Å/10 Å peak ratio (a) and of spacing the (001)-reflection of illite minerals (b).

Fig. 8: Kaolin mineral distribution, mainly kaolinite, plotted as percentage of weighted 7Å peak area component.

Fig. 9: Chlorite distribution, plotted as percentage of weighted 7Å peak area component.

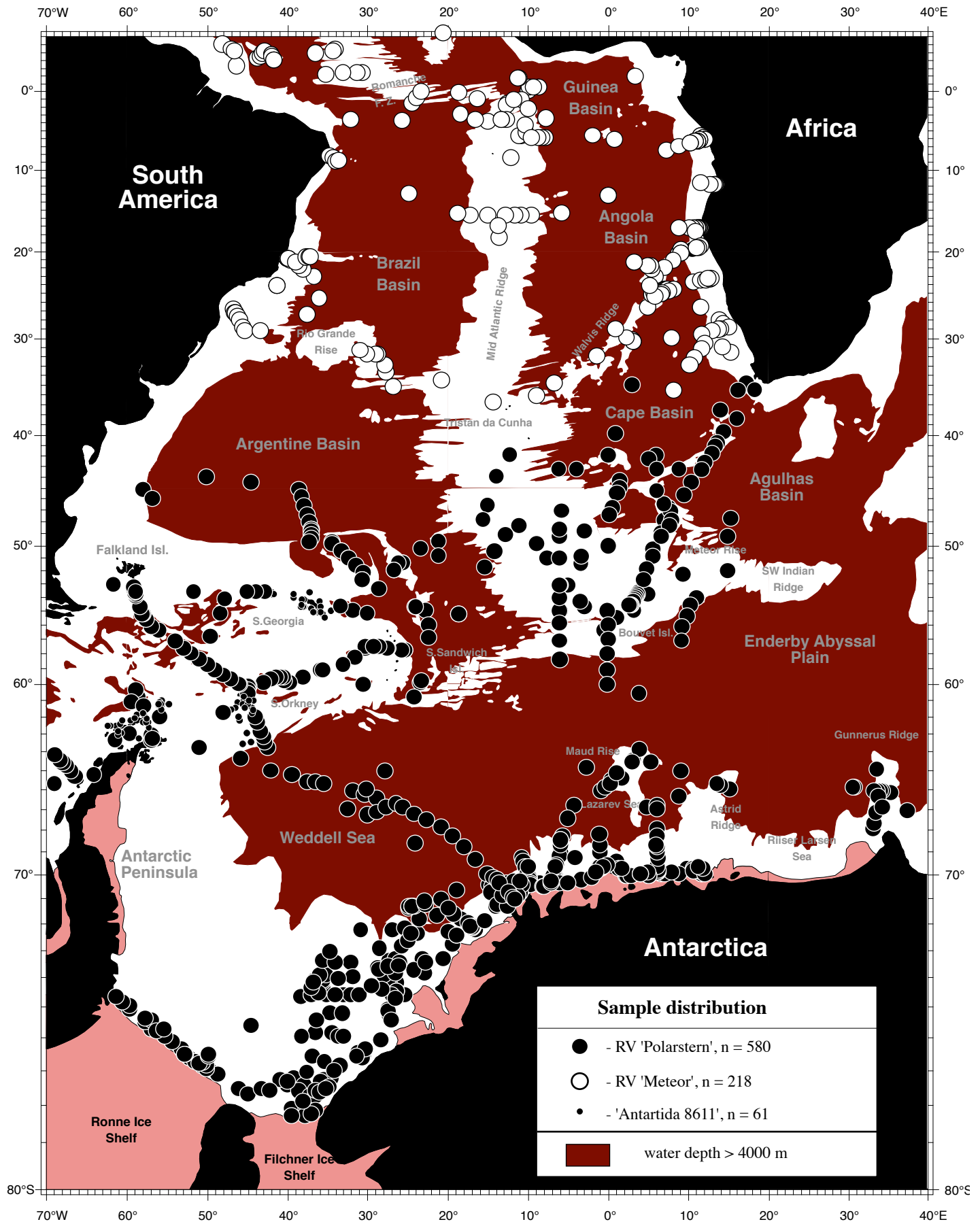
Fig. 10: Kaolinite/chlorite ratios, as computed from the 3.54 - 3.58 Å peak doublet.

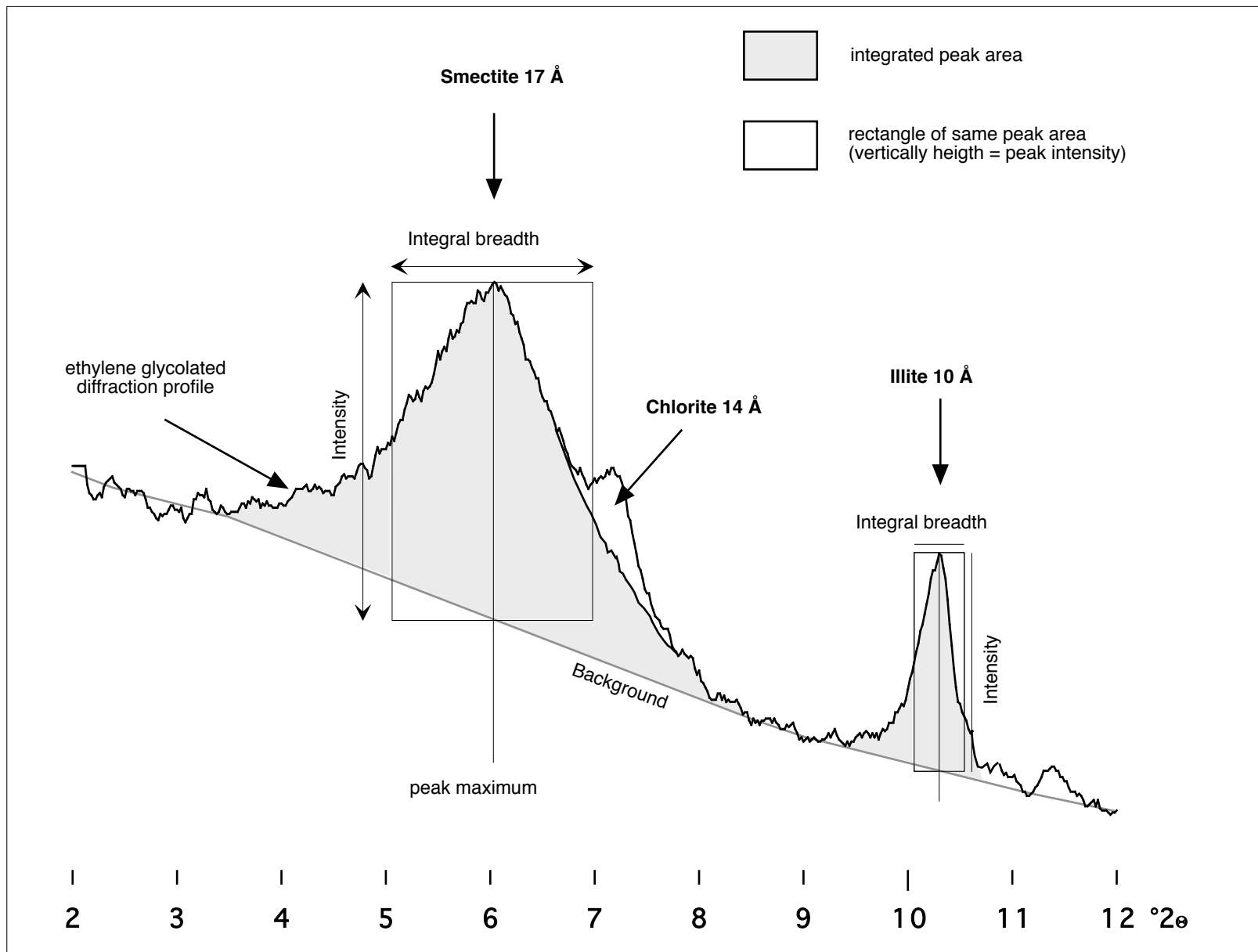
Fig. 11 (a and b): Relation of kaolinite/chlorite ratios to water depth. Samples collected from 20°W to 20°E were projected on the Greenwich meridian from Antarctica to the equator (Fig. 11a). In Fig. 11b the water mass configuration, modified according to Reid (1989) is outlined.

Fig. 12: Characteristic diffraction profiles of the main clay mineral provinces of the South Atlantic.

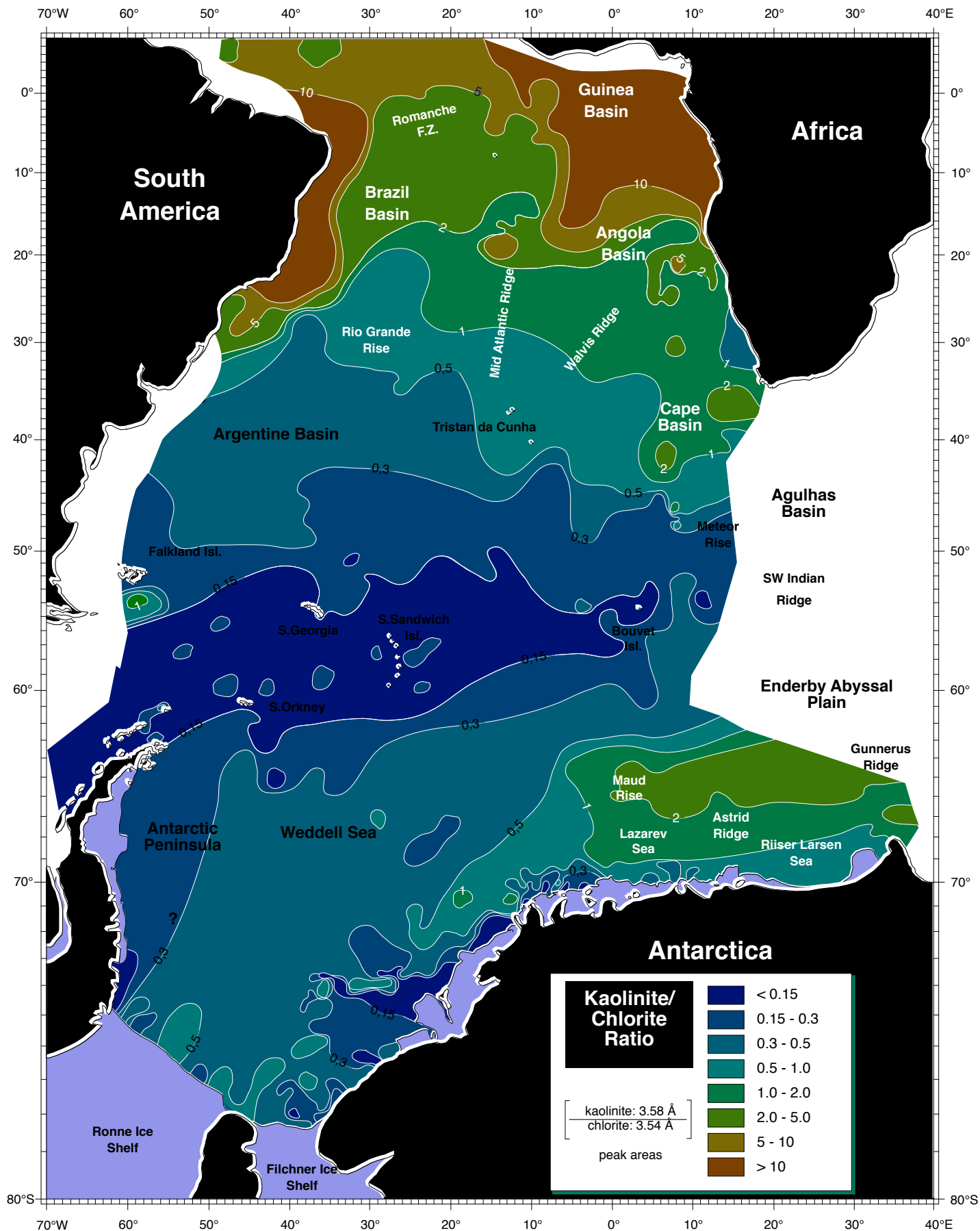
Fig. 13: Simplified map of the main South Atlantic clay mineral provinces. Some of the potential source regions and approximated transport trajectories are indicated by arrows. For signatures refer to table 1.

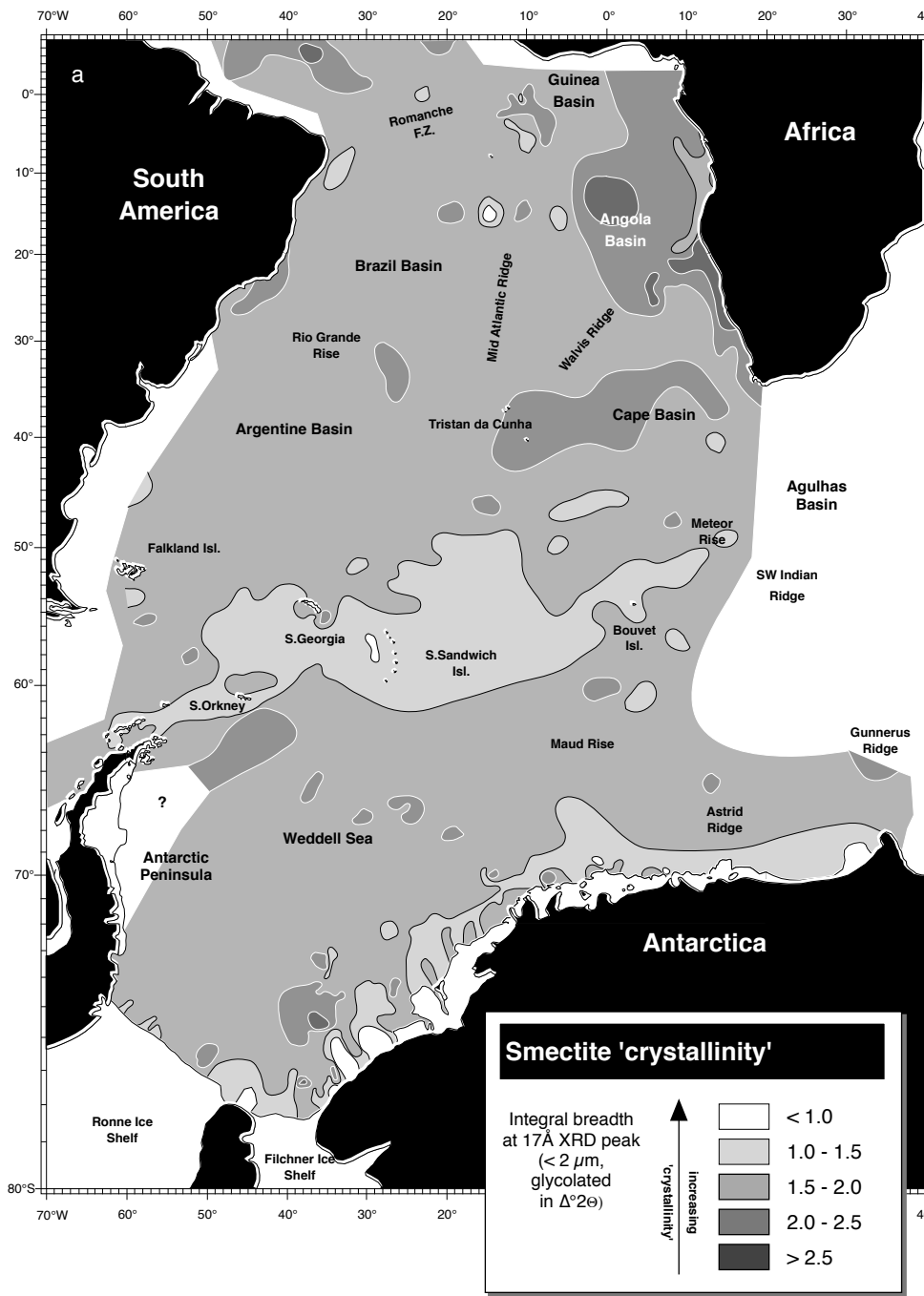
Table 1: The 10 main clay mineral provinces, their typical clay minerals, their source areas and their potential transport media.



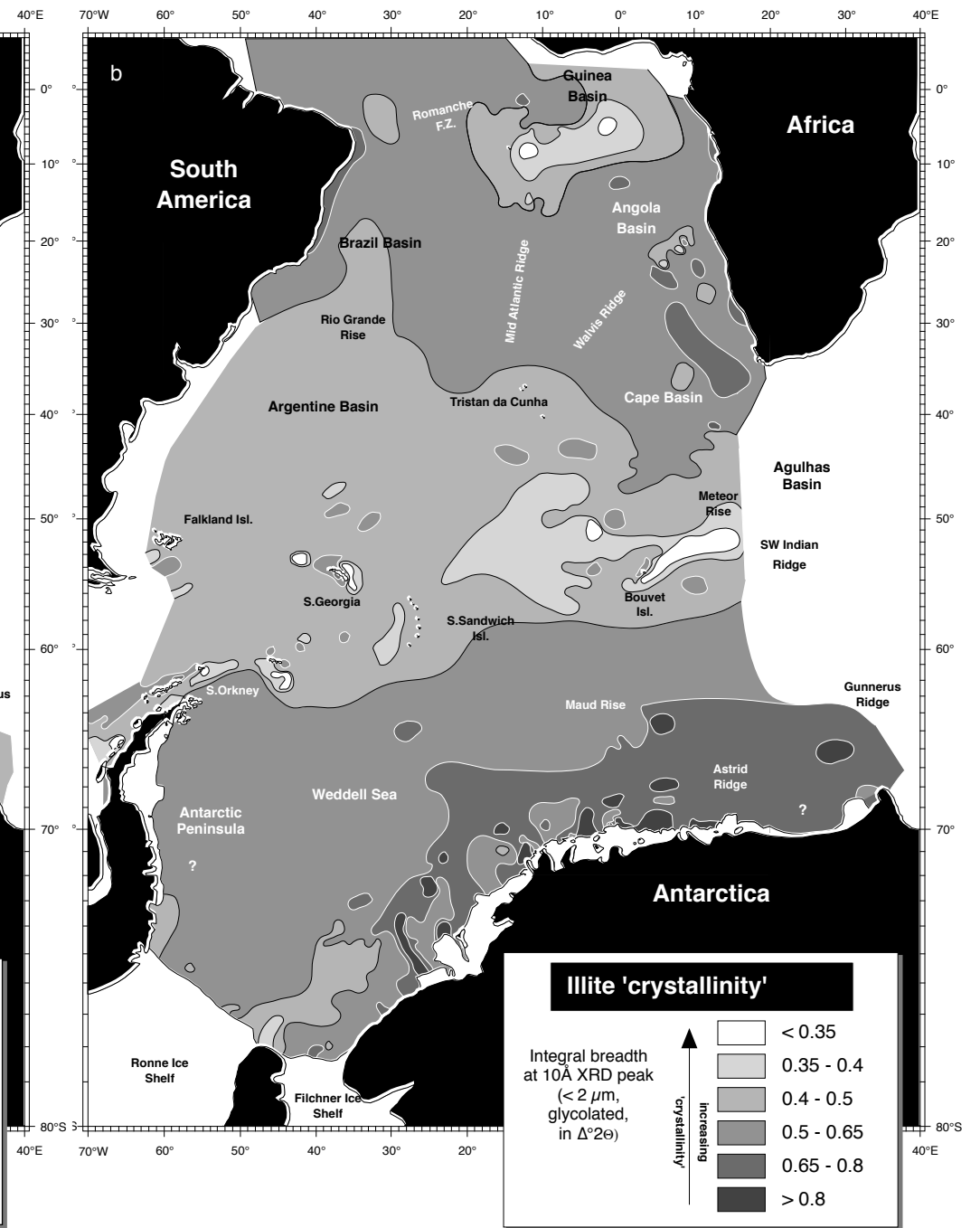


Petschick et al., Fig. 2

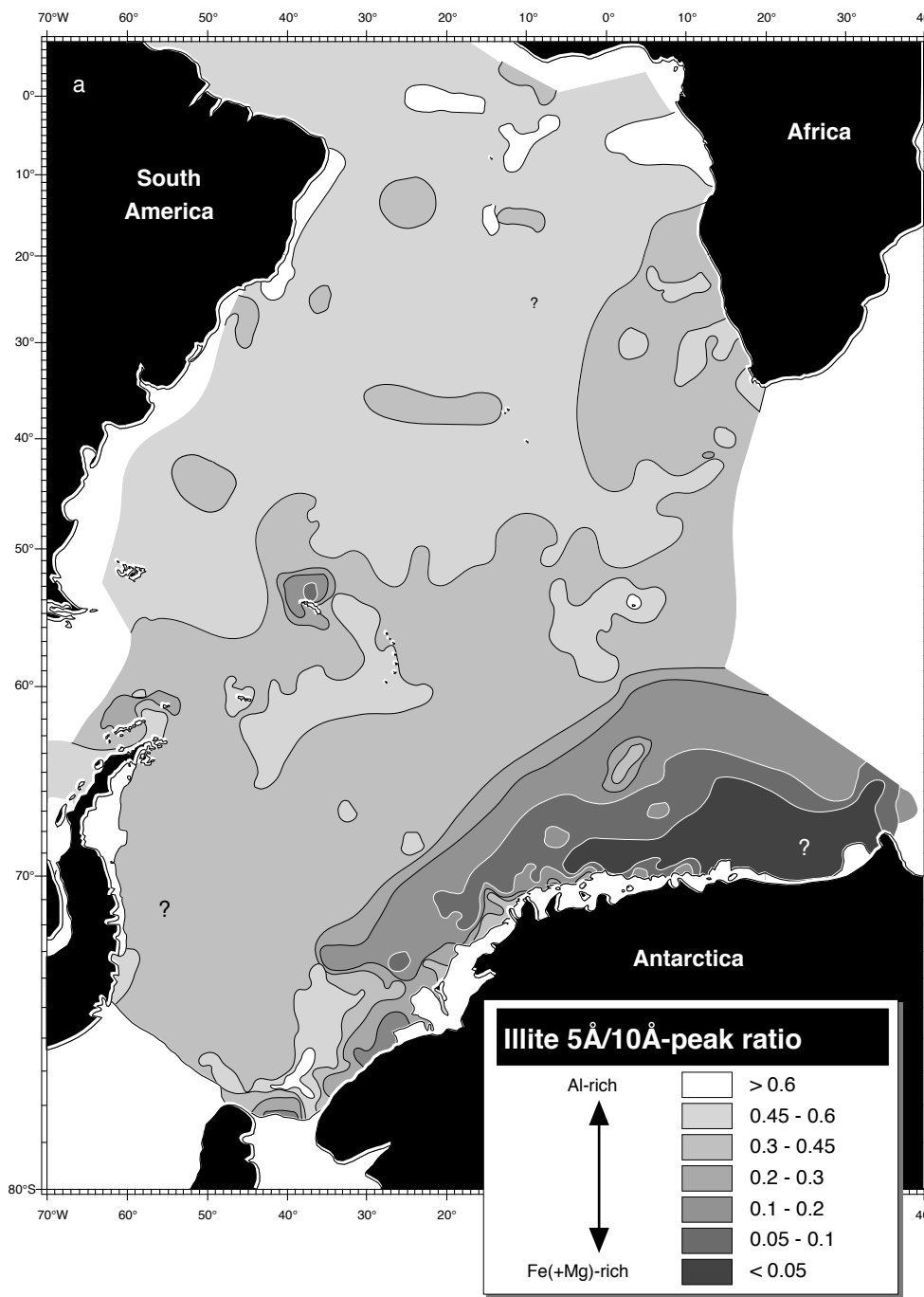




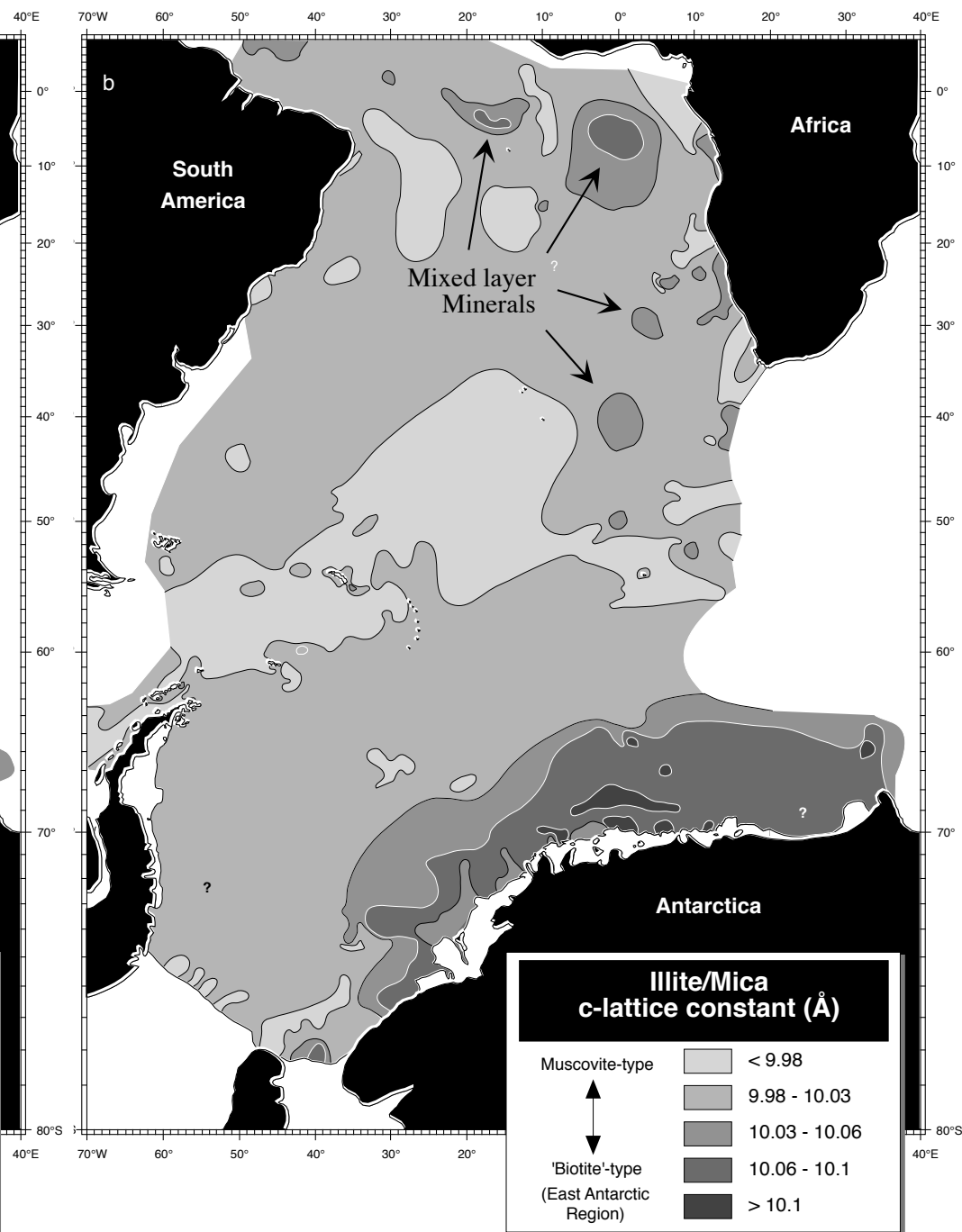
Petschick et al., Fig. 6a



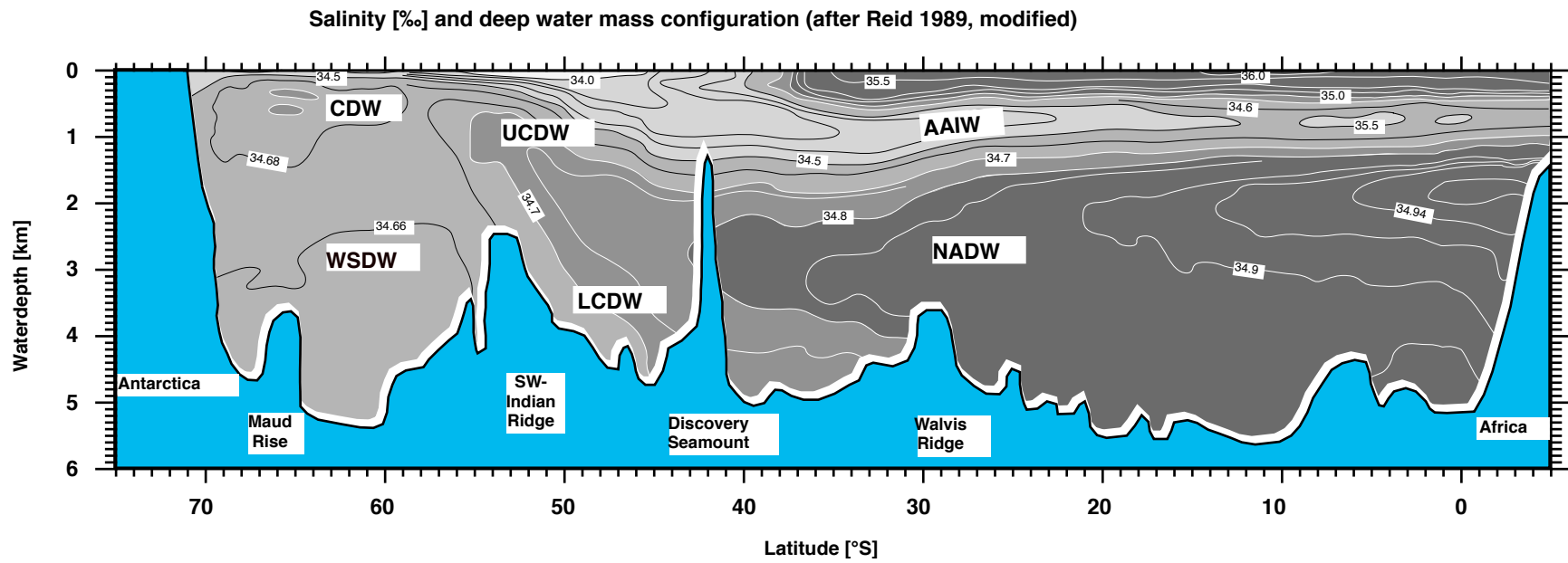
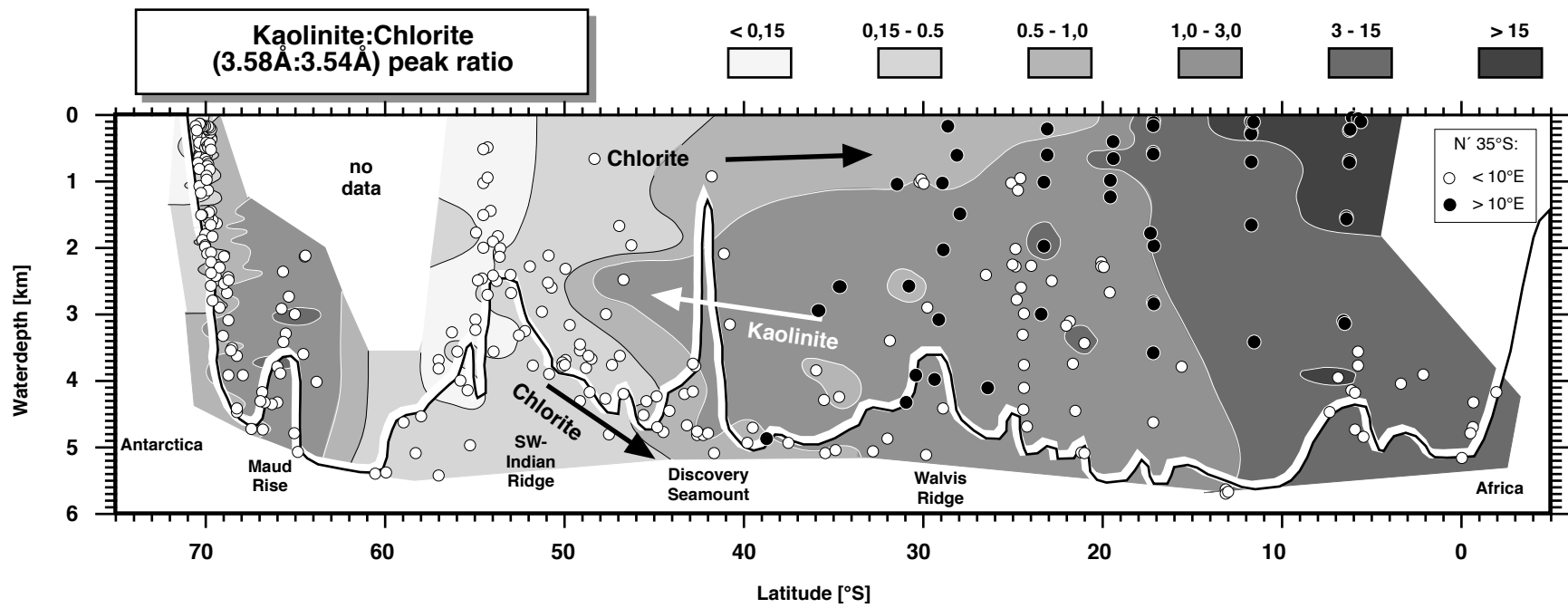
Petschick et al., Fig. 6b



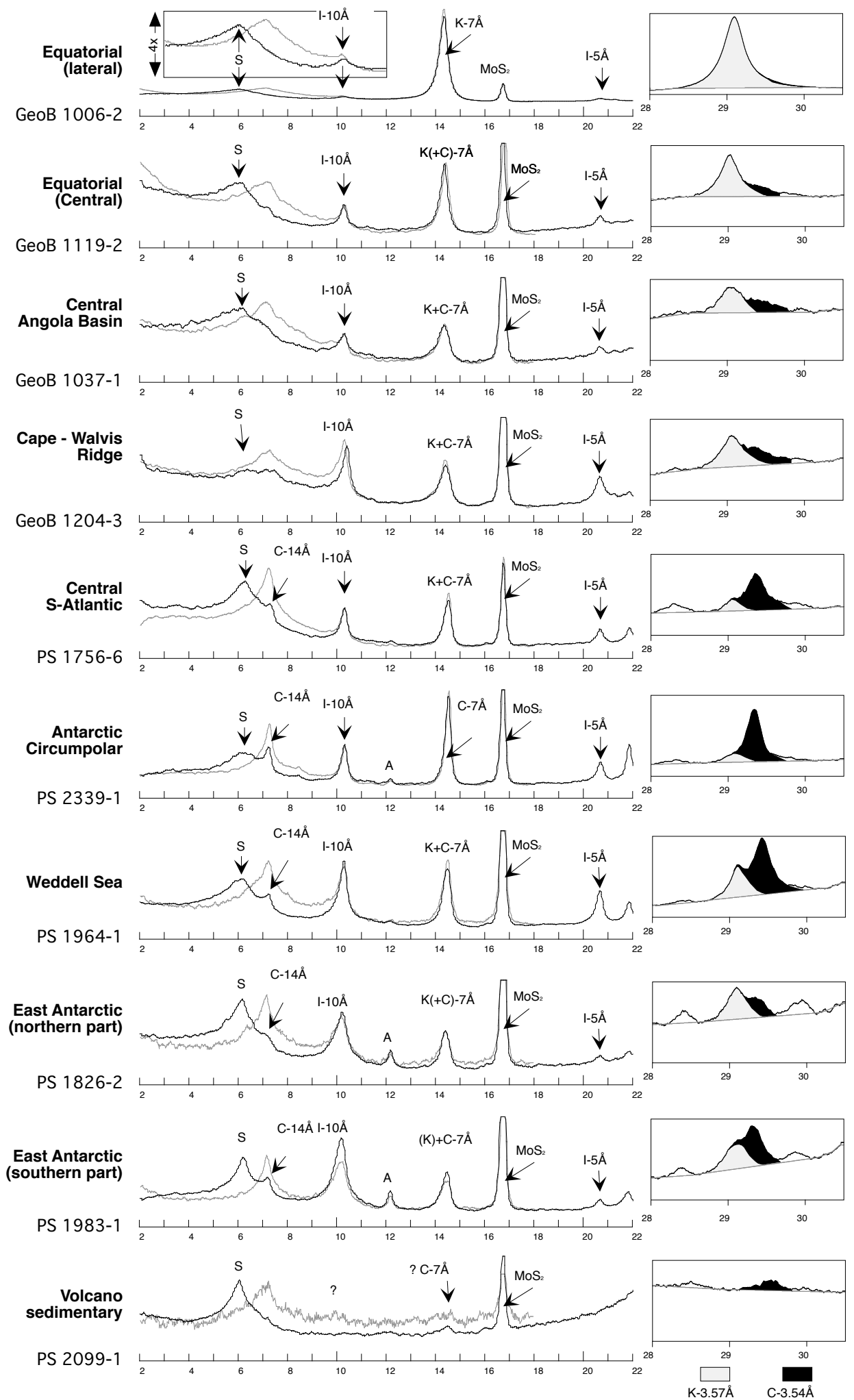
Petschick et al., Fig. 7a

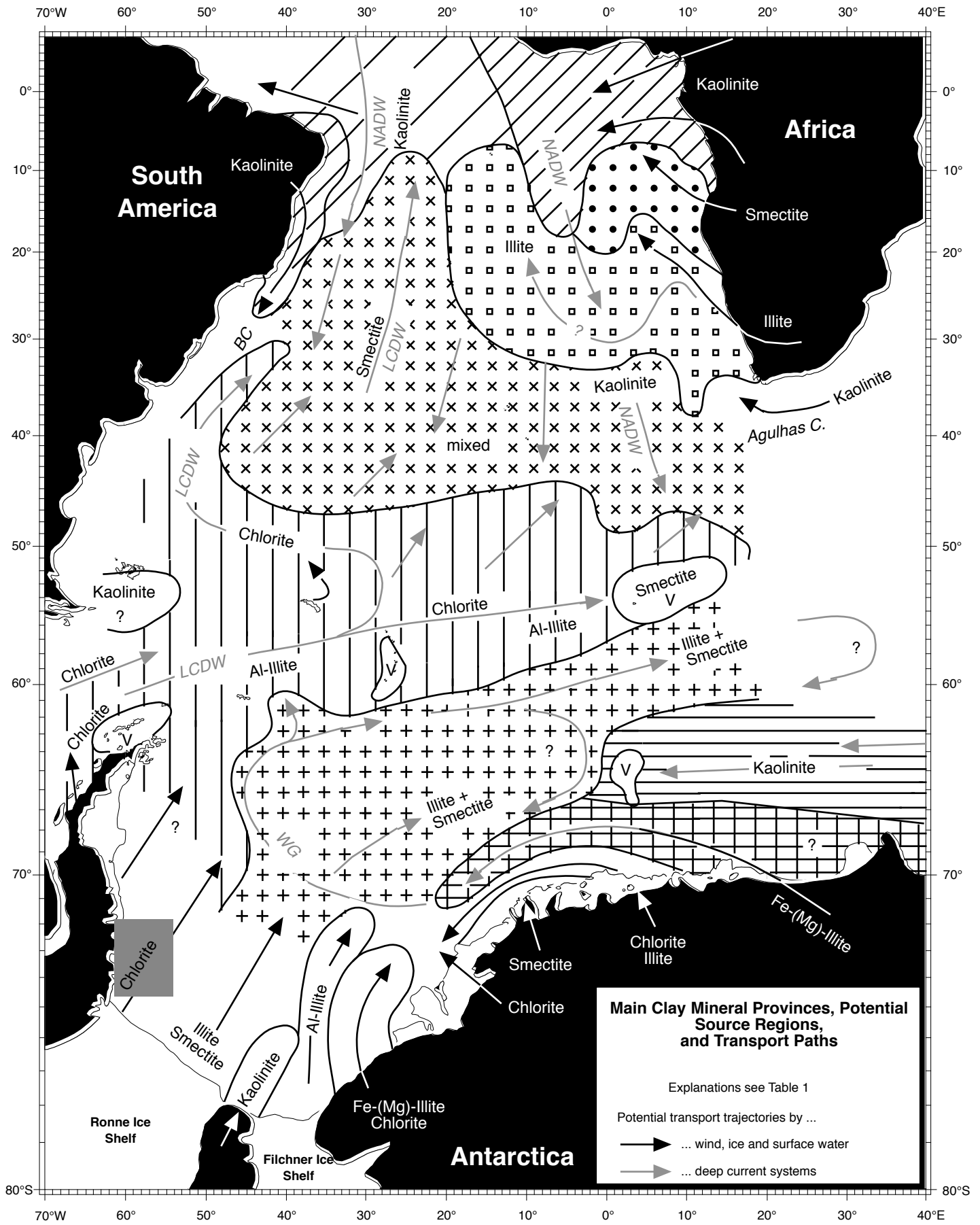


Petschick et al., Fig. 7b

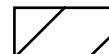
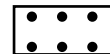
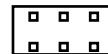
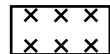
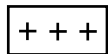
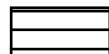
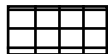


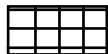
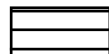
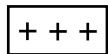
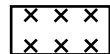
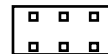
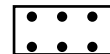
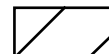
Petschick et al., Fig. 11a and 11b





Symbol in Fig. 13



										
<b>main province:</b>	East Antarctic (southern part)	East Antarctic (northern part)	Weddell Sea	Antarctic Circumpolar	Central S-Atlantic	Cape - Walvis Ridge	Central Angola Basin	Equatorial (Central)	Equatorial (lateral)	Volcanic sediment
<b>typically clay minerals:</b>	Fe-(Mg)-Illite,	Fe-(Mg)-Illite, Kaolinite	Al-Illite, Chlorite, Smectite	Chlorite, Al-Illite, Smectite	Smectite, Illite, Kaolinite, Chlorite	Illite, Kaolinite	Smectite, Kaolinite, Illite	Kaolinite, Smectite, Al-Illite	Kaolinite, Al-Illite	Smectite
<b>main source areas:</b>	E-Antarctica (Illite), Deep Sea Ridges (Kaolinite)	E-Antarctica, Deep Sea Ridges ?	W-Antarctica (Filchner-Ronne Ice Shelf)	Antarctic Peninsula, ? S. Chile and S. Argentina	high diversity by mixing	Southern Africa	Angola	?NW-Africa, N-Brasil	W-Africa, E-Brasil	Deception S. Sandwich Bouvet Islands, Maud Ridge
<b>potential transport media:</b>	Antarctic coastal current	Antarctic coastal current, Weddell Gyre	Weddell Gyre, AABW	CDW and AABW	CDW and NADW	Aerosols, Benguela current, CDW, NADW	Aerosols, Rivers (Kunene) ? NADW	NADW	Rivers (Zaire), Aerosols (Africa), W: Brasil current	-